Shear modulation experiments with ECCD on TCV

S. Cirant 1), S. Alberti 2), F. Gandini 1), R. Behn 2), T.P. Goodman 2), and the TCV Team 2)

1) Istituto di Fisica del Plasma
EURATOM-ENEA-CNR Association, Milano, Italy
2) Centre de Recherches en Physique des Plasmas CRPP EPFL
Association EURATOM-Confédération Suisse
CH-1015 Lausanne, Switzerland

e-mail contact of the first author: cirant@ifp.cnr.it

Abstract Anomalous electron transport is determined by turbulence, which in turn is affected by magnetic shear. A novel application of Electron Cyclotron Current Drive (ECCD), aiming at localized shear modulation, has been applied on TCV tokamak for experiments on shear-dependent electron transport. Pairs of EC beams, absorbed at the same radius but oriented for co and counter injection, are modulated out of phase in order to force a local modulation of current density at constant input power. Off-axis deposition (ρ_{dep}=0.24) is performed for sawteeth control. A significant impact on local shear is achieved with $I_{ECCD}\approx 0.1 I_{OH}$ even if the modulation period is much shorter than current diffusion time. Although source (heat and particle) terms are constant, both electron density and temperature are modulated during alternated ECCD. Thomson Scattering is the diagnostic for local T_e and n_e measurement, in order to overcome suprathermal problems on ECE from high field side. Once equilibrium effects are taken into account for appropriate mapping of TS measurements onto flux coordinates, T_e and electron pressure modulation, peaked on-axis, is confirmed at all radii internal to EC deposition. Best confinement ($\Delta n_{e,0}T_{e,0}$=+12%) is for co-injection, when shear drops from ≈0.5 to less than 0.2.

1. Introduction

The current density profile in a tokamak is a key feature contributing to determine actual discharge thermodynamic quantities through separate but interlinked processes: it controls the relevant geometry by arranging flux surfaces consistently with equilibrium, it provides an heat source term, it determines MHD equilibrium, and it contributes to heat transport by affecting turbulence scale length. Any experimental attempt to study one or the other of these processes has to deal with the difficult task of a clear distinction between them.
Experiments on electron transport with Electron Cyclotron Heating (ECH) are carried out in many machines (AUG, DIIID, FTU, TCV, TS), focussed on the key issue of electron heat transport and its relation with turbulence [e.g.1,2,3]. Since magnetic shear can have an effect on the stability of the modes producing turbulence [4,5,6,7,8,9], clearly the interest in using Electron Cyclotron Current Drive (ECCD) for shear-control, finalized to transport studies, is great. However, this is a typical case in which much attention must be paid to separate heating effects, always present together with ECCD, from transport features. A way to do this is to compare co and counter ECCD in different shots [10]. In earlier times switching from co to cnt was performed within the same shot on the Stellarator Wendelstein VII-AS [11]. A similar procedure has been used in TCV tokamak, suitably tailored to shear modulation by choosing the switching frequency and the absorption radius in order to achieve the largest and most localized perturbation of the current density profile.

2. Experimental set up, practices and diagnostics

Shear-modulation experiments have been performed on TCV by using the ECRH-ECCD system which has recently been completed. It is composed by 9 gyrotrons divided in three clusters. Each cluster is connected to a single high voltage power supply. Two of the clusters each have 3 gyrotrons (82.7GHz, 0.5MW, 2s) used for heating (ECH) and/or current-drive generation (ECCD) in 2nd harmonic X-mode (X2)[12] while the third cluster has 3 gyrotrons (118GHz, 0.5MW, 2s) for top-launch third harmonic X-mode (X3) heating[13]. Two gyrotrons at 82.7 GHz have been used for shear modulation experiments.

The essential aspects of the experimental procedure are as follows: two EC beams, or a pair of beam clusters when available, are oriented toroidally for driving ECCD in opposite directions, and poloidally for having the identical deposition radius r_{dep}. The power is switched on alternatively in the beam clusters by square-wave modulation of the pertaining power supplies at the identical frequency, but exactly out of phase. The power in the two beam clusters is such that the absorbed fraction is identical, so that the instantaneous EC heating is constant and equal to its average value. Because the heat source distribution is constant in time (not modulated), any observed synchronous electron temperature oscillation $\tilde{T}_e$ has to be ascribed to modulation of the transport properties.

In principle, co and cnt deposition layers can be finely overlapped by observing the heat wave excited by each one of the two clusters, the other one being kept CW at half power in order to have the same average absorbed power, and the same average T_e, in all conditions. More difficult is the balancing of the power in the two clusters, to the precision required for revealing small perturbations of thermal diffusivity. In order to take into account all imperfections in power balancing, a preliminary calibration experiment is performed with the same settings (plasma target and EC system) as for the Switching ECCD (SECCD) experiment, but for the toroidal angle which is set for purely perpendicular launch, without any driven current. The residual synchronous oscillations recorded in this calibration experiment provide the reference term to the real SECCD experiment.

Although all main diagnostics (ECE and soft-X emission, FIR interferometer) are used to monitor SECCD effects on electron temperature T_e and density n_e, the detailed quantitative analysis has been performed using Thomson Scattering data, because in this case both T_e and n_e measurements are really local, and taken at the same volume by definition.

Different modulation frequencies from 5 Hz to 70 Hz have been used, but the quantitative analysis discussed in this paper is performed on experiments at 5 Hz for two main reasons: as shown in the following, at this frequency the driven current is a substantial fraction of its steady-state value. Secondly, Thomson Scattering can be used in spite of its relatively low repetition rate of 20 Hz. Nyquist frequency is 10 Hz in this case, allowing FFT analysis of the 5 Hz modulated signals.

Experimental information on the current density profile is provided by the estimate of the internal inductance and by MHD activity, mostly by sawtooth. The diamagnetic loop is used to confirm appropriate power balancing between the two beam clusters.

Finally, it should be noted that stationary periodic perturbations allow the use of well-known techniques of synchronous detection with much greater sensitivity than in purely transient or steady-state conditions. In fact, the discussion in the following will be entirely based on amplitude and phase of oscillations (any quantity) at the fundamental switching frequency.

3. Steady periodic alternate ECCD and electrodynamic effects on magnetic shear

Because of the transient nature of SECCD, localized in a narrow layer inside a conductive medium, the elctrodynamic plasma response must be taken into account in the estimate of the actual distribution of the driven current. By taking advantage of the periodicity of the equivalent e.m.f. locally applied by SECCD, we follow a simplified procedure for calculating the periodical amplitude current distribution. Instead of solving the complete current diffusion equation, we imagine the plasma composed by N toroidal shells mutually coupled, with an e.m.f. assigned to each shell accordingly to the calculated ECCD (TORAY, Fig.3). The periodical current distribution I_n, n=1:N, is provided by solving a system of linear circuit equations.

In order to get a reliable evaluation of the periodic modification of the shear profile, all sources of modulated current must of course be taken into accounts. We anticipate here the observation, thoroughly discussed in following sections, that the electron temperature is modulated during SECCD, which creates a modulated current drive term to be added to SECCD. From the electrodynamic point of view the change in resistivity is equivalent to the application of an additional, distributed "current drive" $J_{\eta}(\rho) = (\Delta\eta/\eta)J(\rho)$, where $\Delta\eta/\eta$ is the relative change in resistivity and $J(\rho)$ is the average current density profile. Figure1 summarizes the results of a simulation of shot #24867. Total ECCD current is 12 kA, peaked at 5.7 cm, 3.1 cm wide (1/e^2 of the peak value). Resistive current drive is peaked at center, it has a width of 5 cm, with a total modulated current of 12 kA. Swing frequency is 5 Hz. Main thing to be noted is that electrodynamic reaction to ECCD is strong, but a large fraction of localized current drive still persists, with a significant modulation of the current density profile . Magnetic shear modulation is therefore evident near r_{dep} (±60%, from 0.15 to 0.75 min to max).

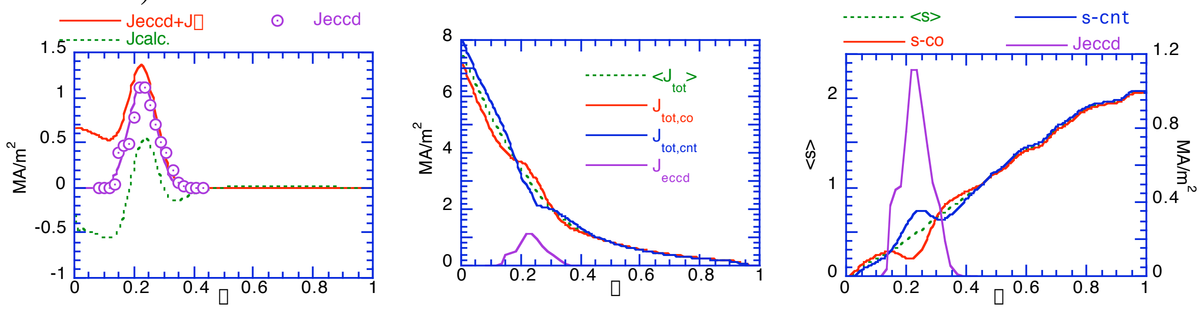

Fig.1 –Left: Total driving term, ECCD (dots) and resistive (solid line), is shown with the oscillating current amplitude (dashed), determined by electrodynamic reaction. Center: total current density, average (dashed), during co (red) and counter (blue) injection period. Right: magnetic shear profile.

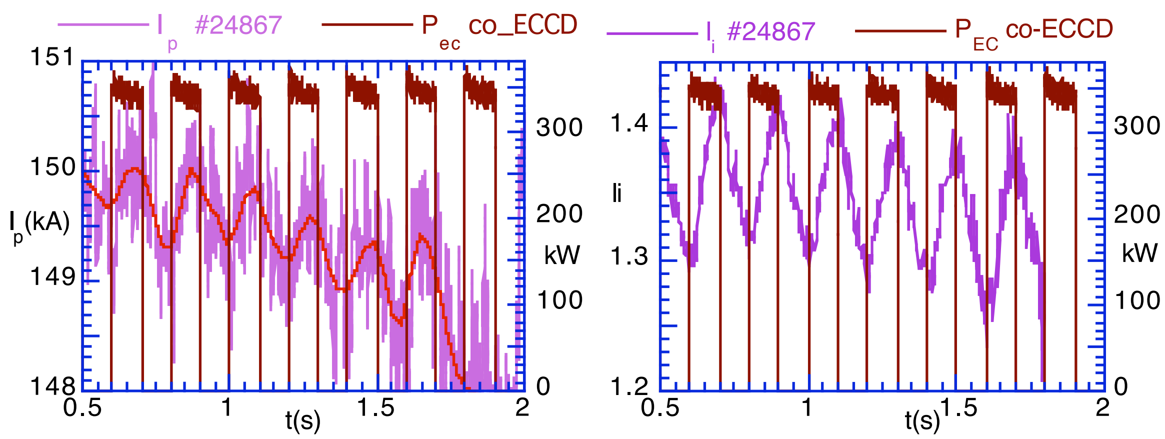

Fig.2 – Internal inductance (right), compared with EC power in the beam oriented for co-ECCD injection. Left figure shows plasma current oscillations, in-phase with the internal inductance and with co-ECCD.

An experimental validation of calculated current profile changes $\tilde{J}(\rho)$ is given by the internal inductance time evolution. Fig.2, left, shows the power from the gyrotron $P_{EC,co}$ dedicated to co-ECCD, and the plasma current oscillating correspondingly (with appropriate phase shift).

The internal inductance increases during the co-injection phase (Fig.2, right), consistent with the calculated flattening of the current density profile (Fig.1, center).

The change in internal inductance, due to both SECCD and resistivity oscillations, is $\Delta l_i = 3.1\%$, very close to the measured value of 3.4%. In addition, a loop voltage (periodical) of V_ϕ =20 mV is calculated, very close to the measured value of 24 mV, with a very good agreement also between measured and calculated I_ϕ-V_ϕ phase delay.

Furthermore, sawteeth are suppressed during the co-injection phase (gyrotron 2), and re-appear during the cnt-injection phase (gyrotron 5). During cnt-injection the magnetic shear is strongly increased at r_{dep}, and the safety factor is slightly reduced inside r_{dep}. In the case of co-injection the opposite holds true. Both strong shear near to q=1 surface (note that $\rho_{inv} \approx 0.13 \approx \rho_{dep}$, which is the most effective arrangement for affecting sawteeth with ECH/ECCD) and low central q are destabilizing factors for sawteeth [14]. This is important experimental evidence supporting the claim that ECACD drives a modulation of the current density profile as foreseen and calculated.

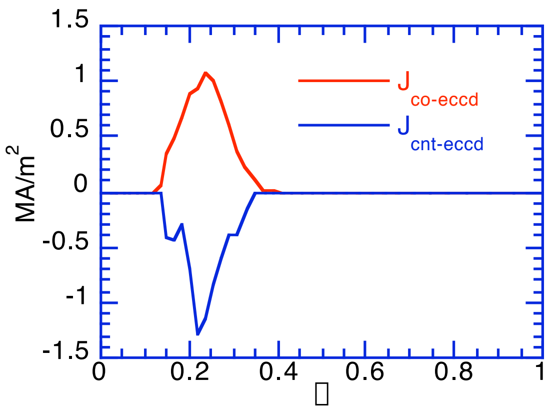

Fig.3 – Current density profile for co (red) and counter (blue) injection, calculated from linear ECCD theory (TORAY code).

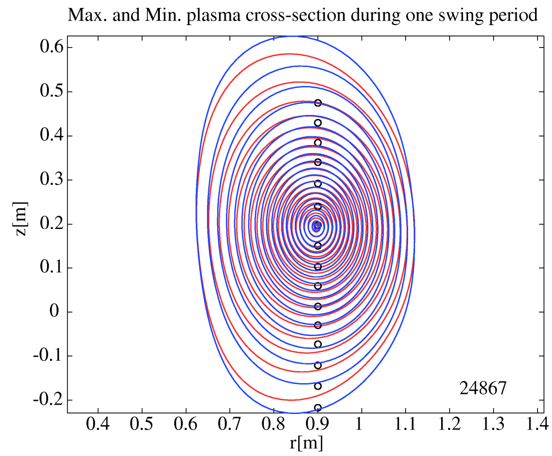

Fig.4 – Magnetic flux surfaces for co and counter injection. Dots mark the position of Thomson Scattering measurements.

4. Electron temperature modulation at constant heating power

The essential feature of swing ECCD experiments is that, in principle, the instantaneous EC heating power is constant. Any detectable $\tilde{T}_e$ synchronous fluctuation can be ascribed therefore to a modulation of heat confinement, possibly induced by SECCD. Effective $\tilde{J}(\rho)$ modulation might cause synchronous modulation of the whole equilibrium frame, as indeed observed (Fig.4). Since the grid of Thomson Scattering measuring points is fixed in the laboratory frame, this effect clearly must be taken into account. The electron density must be monitored and, in case of modulation, properly taken into account. A whole section will be dedicated to this point in the following

The striking feature (shot #24867) is that T_e strongly oscillates (more than 30% peak-to-peak at centre) in spite of constant input power. Fig.5 and Fig.6 show the main features of this internal heat wave. The whole T_e profile oscillates internal to the EC wave absorption radius r_{dep}. A thermal barrier (or a step-up in thermal diffusivity) is alternated at r_{dep} to a thermal bridge (or a step-down in diffusivity), in synchronism with ECCD. The phase distribution of the oscillations, Fig.6, confirms that the modulation is generated in the plasma core, internal to r_{dep}, and propagates outwards. If local transport is modulated, important effects should be found in ∇T_e also. ∇T_e can be modulated either because local diffusivity χ_e is modulated at constant heat flux Φ, or because the heat flux itself oscillates. Since $n_e \nabla T_e = -\Phi/\chi_e$, and assuming that n_e is constant, we get:

$$\frac{\nabla \tilde{T}_e}{\nabla T_{e,0}} \approx \frac{\tilde{\Phi}}{\Phi_0} - \frac{\tilde{\chi}_e}{\chi_{e,0}}$$

where $\nabla \tilde{T}_e$ is the amplitude of the oscillating gradient (obtained by FFT analysis of the incremental ratio of the T_e data), and $\nabla T_{e,0}$ is the gradient of the averaged profile. All other quantities have a similar meaning. $\tilde{\Phi}$ is partly due to a sloshing flux possibly caused by re-adjustments of χ_e, vanishing on a time scale longer than local heat transfer time constant. Its contribution to fluctuating gradient is expected therefore to be negligible.

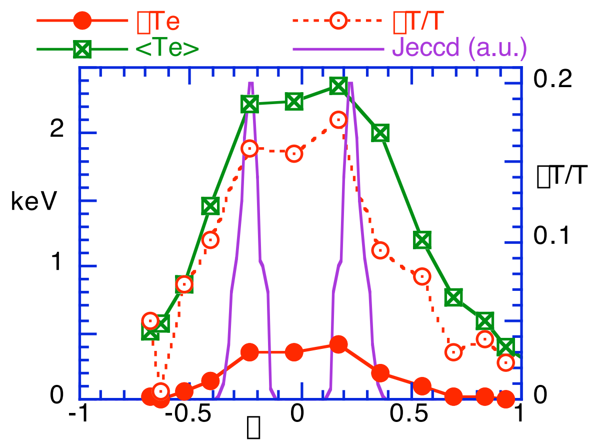

Fig.5 – Red full dots: amplitude of T_e oscillations synchronous to swinging. Green crossed squares: averaged T_e profile. Open red dots: relative change.

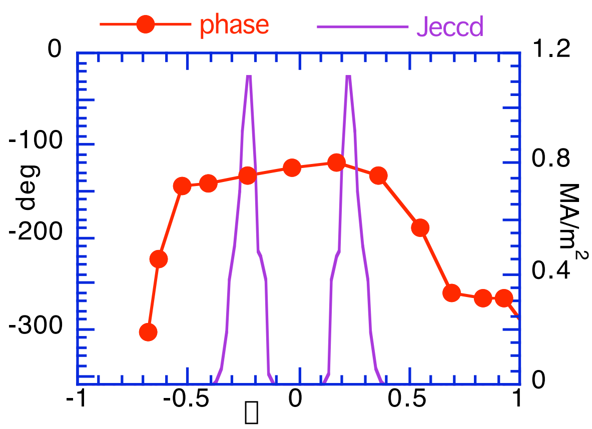

Fig.6 – Red full dots: phase of T_e oscillations synchronous to swinging. The ECCD profile (violet) is shown in both Fig.5 and Fig.6

The main contribution to $\tilde{\Phi}$ is due to a feed-back from χ_e which modulates T_e, which modulates (in phase opposition to $\tilde{T}_e$) the ohmic input. We assume therefore that:

$$-\frac{\tilde{\chi}_e}{\chi_{e,0}} \approx \frac{\nabla \tilde{T}_e}{\nabla T_{e,0}} - \frac{\tilde{\Phi}_{oh}}{\Phi_{oh,0}}$$

The measured $\nabla \tilde{T}_e / \nabla T_{e,0}$ (FFT on T_e incremental ratio) and the relative heat flux modulation $\tilde{\Phi}_{oh}/\Phi_{oh,0}$, estimated on the basis of observed T_e fluctuations and assuming Spitzer resistivity, are shown in Fig.7. Outside r_{dep} the relative change of the gradient is fully explained by heat flux modulation. This is not the case in the whole region at r_{dep}, where gradient fluctuations are twice the flux oscillations. This implies that $\tilde{\chi}_e/\chi_{e,0}$=0.5 at r_{dep}. Inside r_{dep} both $\nabla \tilde{T}_e$ and $\nabla T_{e,0}$ are small, and the error in the measure prevents a reliable estimate of their ratio. However, the absence of a phase delay and of a damping of the heat wave at center with respect to r_{dep} supports the conclusion that transport is modulated in the whole region internal to r_{dep}. It has to be noted that T_e increases, and transport drops, during the co-injection phase, when shear is also low (Fig.8). The same result is obtained by the estimate of χ_e with power balance analysis. Fig.9 shows that $\chi_{e,PB}$ (at ρ=0.2) is modulated out of phase with respect to T_e, and in phase with magnetic shear modulation.

Consistent with χ_e modulation, a modulation of the global energy content W_e is also observed. The observed relative change $\tilde{W}_e/\langle W_e \rangle$=0.04, confirmed by 4% oscillation amplitude measured in the diamagnetic signal, is compatible with a 40% change in electron diffusivity over a volume smaller than 25% of the total one, considering also that in the meantime in the same volume there is a loss of 40% in ohmic heating (modulated T_e). Global energy confinement behaviour is therefore consistent with the observed modulation of local thermal diffusivity.

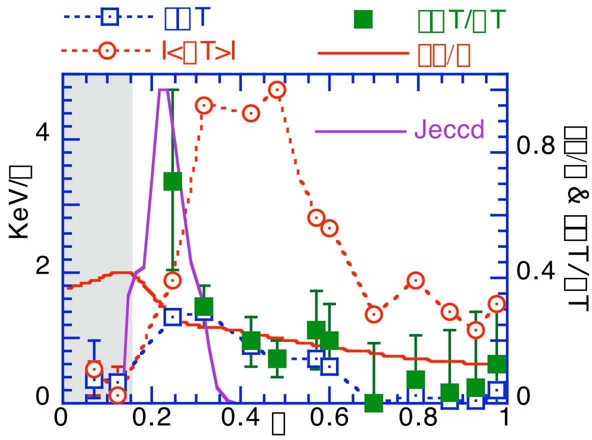

Fig.7 –∇T_e is the average T_e gradient, and $\delta\nabla T_e$ is the periodic component. Same meaning for of heat flux q and δq.

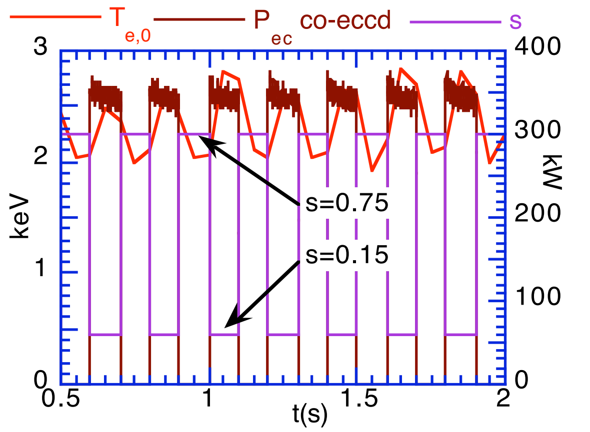

Fig.8 – $T_{e,0}$ (red) and confinement increase during the co-injection phase (P_{ec}), when shear s is the lowest.

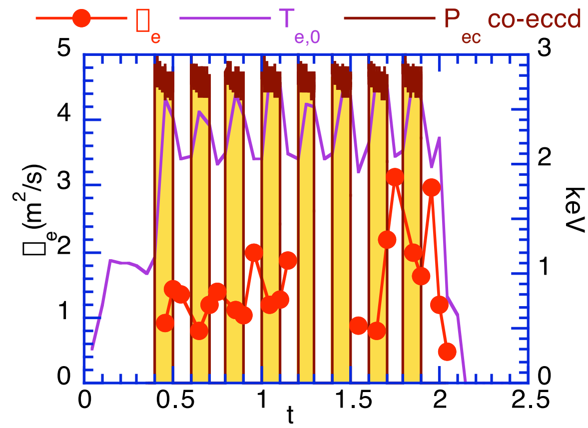

Fig.9 – In addition to the peak temperature and the EC power driving current in the co-direction, the figure shows the time dependence of the electron thermal diffusivity from power balance.

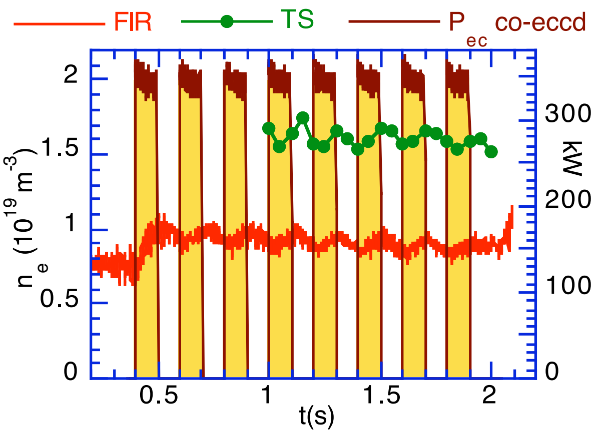

Fig.10 – Electron density from FIR interferometer, central chord, and from Thomson Scattering. P_{ec} for co-injection provides, as in the other figures, the time frame.

It has to be noted that $\tilde{T}_e$ modulation caused by χ_e is opposed by modulation of the ohmic input. At constant input power, the temperature change would have been much larger.
All the elements of thermal analysis converge to the point that a local decrease (≈60%) in the magnetic shear determines a decrease of the same amount (≈40%) in the electron thermal diffusivity at and inside r_{dep}.

5. Electron density modulation at constant particle sources

Although particle sources are likely constant during SECCD, electron density n_e is clearly modulated during these experiments. Since the equilibrium is modified with SECCD, we need to take this into account, as in the analysis of electron temperature. However unlike the T_e measurement, changes in n_e measurements might be due not only to motion of Thomson Scattering (TS) observation point across magnetic surfaces, but also to thickening/rarefaction of flux surfaces at the same point, causing reduction/increase of the volume between surfaces.

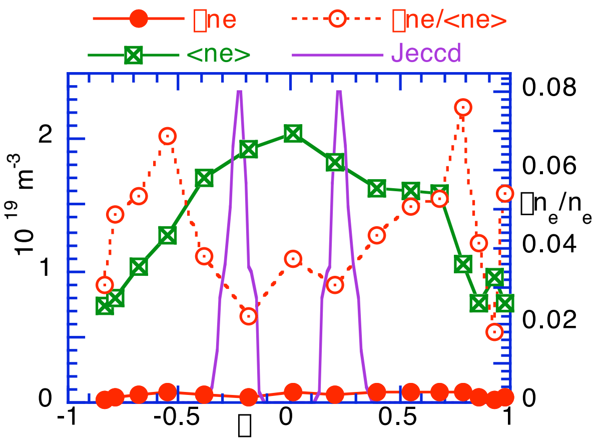

Fig.11 – Red full dots: amplitude of n_e oscillations synchronous to swinging. Green crossed squares: averaged n_e profile. Open red dots: relative change.

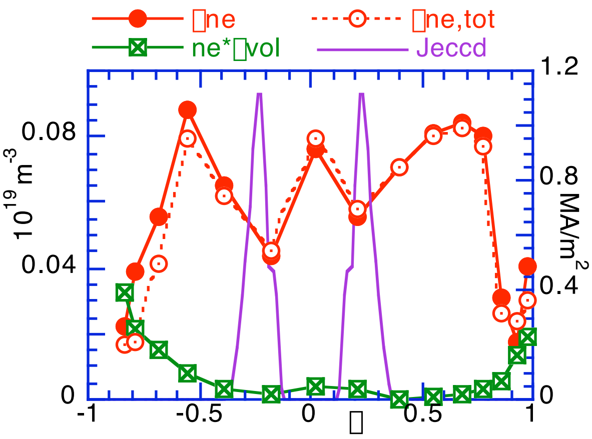

Fig.12 – Full dots: density oscillations. Crossed squares: δn_e due to volumetric effects. Open dots: total δn_e, corrected by equilibrium and volumetric effects.

Figure11 summarizes the results of the analysis of synchronous density oscillations performed by FFT of the TS density data corrected by equilibrium modulation (but not by volumetric effects). Density oscillation amplitudes are small (only a few percent), but outside the error bar given by the random noise in the FFT spectra. Figure 12 shows that the correction term due to volumetric effects is even smaller, densification/rarefaction of flux surfaces being peaked at the plasma periphery. It follows that we can neglect equilibrium volumetric effects on the density modulation.

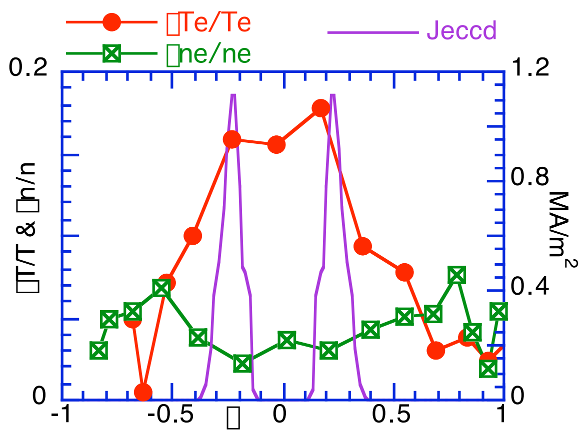

Fig.13 – Relative amplitude of T_e and n_e oscillations synchronous to swinging. Both data are corrected for equilibrium modulation effects. The ECCD profile is shown for reference

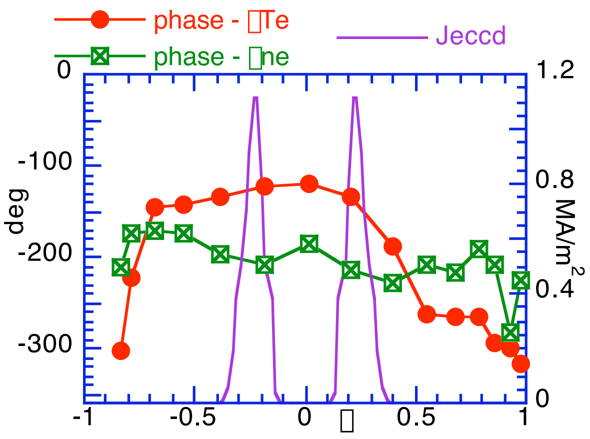

Fig.14 – Red full dots: phase radial profile of T_e oscillations synchronous to swinging. Green crossed squares: phase of n_e oscillations. Both data are corrected for equilibrium modulation effects.

If we compare amplitude and phase of T_e and n_e oscillations (Fig.13 and 15), we see that the two effects are both determined by SECCD, but as a result of different processes. $\tilde{T}_e$

oscillations are limited in the region inside the deposition radius, and possibly propagate outwards, while $\tilde{n}_e$ oscillations are originated in a broader region extending outside the deposition radius. The phase is also quite different in the two cases, confirming that different processes are going on in the two regions.
Because of the small relative amplitude of $\tilde{n}_e$, we can neglect their impact on $\tilde{T}_e$.

6. Conclusions

Electrodynamic calculations show that ±40% (from 0.15 to 0.75) shear modulation can be achieved at r_{dep} in Switching ECCD experiments on TCV. Shear modulation is localized at the CD layer. Internal inductance measurements and sawteeth activity evolution support the calculations.

In spite of the constant heating power, the presence of electron temperature oscillations show that electron transport is modulated at, and possibly inside, the SECCD layer. The observed ±40% relative amplitude of χ_e modulation is at the same level of the shear modulation amplitude.

An important result is that electron transport is reduced when shear is low. This provides useful information on the issue of magnetic shear destabilization of drift-waves [e.g. 4], and on the link between transport and fine-scale turbulence.

Small amplitude density oscillations are also observed during SECCD, although a process different from energy confinement is acting, possibly related to the $n_e(q)$ functional dependence.

Acknowledgement: This work was partially supported by the Swiss National Science Foundation

References

[1] F.Ryter, Nucl. Fusion **43** (2003) 1396–1404
[2] C Gormezano, Plasma Phys. Control. Fusion **41** (1999) B367–B380.
[3] Ulrich Stroth, Plasma Phys. Control. Fusion **40** (1998) 9–74
[4] A. Kendl and B. Scott, 29th EPS Conference on Plasma Phys. and Contr. Fusion Montreux, 17-21 June 2002 ECA Vol. **26B**, P-3.211 (2002)
[5] JW Connor and R J Hastie, Plasma Phys. Control. Fusion **46** (2004) 1501–1535
[6] F Jenko and A Kendl, New Journal of Physics 4 (2002)
[7] F Jenko and W Dorland, Plasma Phys. Control. Fusion 43 (2001) A141–A150
[8] B.D. Scott, Phys. Rev. Lett. 65, 3289 (1990)
[9] B.D. Scott, Plasma Phys. Contr. Fusion 39, 1635 (1997)
[10] R.C. Wolf, Nuclear Fusion, Vol. **41** (2001) 1259
[11] V.Erckmann et al., IAEA Proc.1995, Plasma Physics and Contr. Nuclear Fusion Research, Vol.1, p. 771-781, paper IAEA-CN-60/A6-3
[12] T. Goodmann et al., Fusion Technology (Proc. of 9th Symp. Lisbon 1996), North-Holland, Amsterdam (1997), 565.
[13] J.P. Hogge et al., Proc. of 12th Joint Workshop on ECE and ECRH, Aix-en Provence, France 2002, p.371.
[14] G.Ramponi et al., RADIO FREQUENCY POWER IN PLASMAS, 13th Topical Conference, Annapolis, Maryland (USA), April 1999, AIP Conf. Proc. 485 , 265 (1999)